

# Calorimetric and Neutron Diffraction Studies on Transitions of Water Confined in Nanoporous Copper Rubeanate

Takeshi Yamada,<sup>†,§</sup> Ryo Yonamine,<sup>†</sup> Teppei Yamada,<sup>‡,§</sup> Hiroshi Kitagawa,<sup>‡,§,⊥</sup> and Osamu Yamamuro<sup>\*,†,§</sup>

*Institute for Solid State Physics, University of Tokyo, 5-1-5 Kashiwanoha, Kashiwa, Chiba 277-8581, Japan, Graduate School of Science, Kyusyu University, 6-10-1 Hakozaki, Higashi-ku, Fukuoka 812-8581, Japan, Graduate School of Science, Kyoto University, Oiwakecho, Kitashirakawa, Sakyo-ku, Kyoto 606-8502, Japan, and JST-CREST, Japan*

*Received: December 28, 2009; Revised Manuscript Received: May 12, 2010*

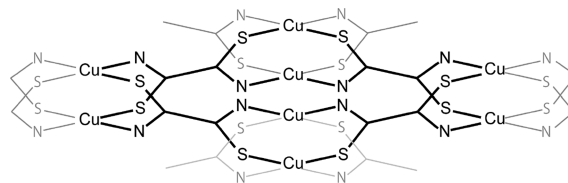
Copper rubeanate ( $\text{H}_2\text{C}_2\text{N}_2\text{S}_2\text{Cu}$ ) has a nanoporous structure and exhibits high proton conductivity with adsorbing water inside the pores. We have studied the phase behavior and structure of the water confined in copper rubeanate hydrates ( $\text{H}_2\text{C}_2\text{N}_2\text{S}_2\text{Cu} \cdot n\text{H}_2\text{O}$ ,  $n = 0, 2.1, 3.7$ ) by adiabatic calorimetry and neutron powder diffraction. In the hydrate samples, a glass transition and a first-order transition appeared around 150 and 260 K, respectively. The transition entropy was similar to the entropy of fusion of bulk water, indicating that the adsorbed water is disordered above the transition temperature, like bulk water, and ordered below 150 K, like bulk ice. The neutron diffraction data demonstrated that both dry and hydrated copper rubeanates have amorphous structures over the temperature range 100–340 K. The analyses on the diffraction peak owing to the adsorbed water revealed that the transition at 260 K is a liquid–liquid transition due to the condensation of water on the surface of the pores, and the condensed water molecules are gradually ordered below 260 K and frozen-in at the glass transition around 150 K.

## I. Introduction

Water, which is the most common liquid in our life, is a very unusual liquid from the viewpoint of physical chemistry. For example, the density of water has a maximum at 4 °C, and on further cooling the heat capacity, thermal expansivity and isothermal compressibility increase and tend to diverge below 235 K.<sup>1</sup> The recent approach taken to explain these anomalies involves the existence of a transition between low-density water (LDW) and high-density water (HDW) hidden in an inaccessible supercooled regime below 235 K.<sup>2,3</sup> This idea is based on the experimental evidence of a first-order transition between low-density amorphous ice (LDA) and high-density amorphous ice (HDA) found by Mishima at ~135 K.<sup>4</sup> Soper and Ricci actually reported a continuous transformation between LDW and HDW by a neutron diffraction experiment at 268 K, which is above the critical temperature of the LDW–HDW transition, under high pressure ( $0 < p < 400$  MPa).<sup>5</sup> Since water inevitably crystallizes at the homogeneous nucleation temperature 235 K, the LDW–HDW transition is usually investigated by using nanoporous materials in which crystallization of water is suppressed by the surface effect, size effect or both.

There are various nanoporous materials: for example, porous silicates (MCM-41, FSM-16, etc.), zeolites, carbon nanotubes, etc. Liu et al. reported quasi-elastic neutron scattering<sup>6</sup> in which the temperature dependence of the translational relaxation times  $\tau$  of water confined in MCM-41 gave a kink around 225 K. The temperature dependence of  $\tau$  is Arrhenius below 225 K but non-Arrhenius above 225 K. Therefore, they assert that this

## SCHEME 1: Chemical Structure of $\text{H}_2\text{dtoaCu}$



anomaly is due to the transition between LDW of a strong liquid and HDW of a fragile liquid. Yoshida et al. obtained a similar result for deuterated water confined in MCM-41 by using neutron spin echo.<sup>7</sup> Chu et al. observed a similar strong–fragile transition in water confined in carbon nanotubes.<sup>8</sup> Adiabatic calorimetry by Oguni et al.<sup>9</sup> showed that the fusion of water confined in silica gels was broader in shape, and its characteristic temperature decreased with decreasing pore diameter. In the sample with the smallest pore diameter (1.1 nm), a hump in the heat capacity appeared at 227 K due to a liquid–liquid transition. They also found two glass transitions, each attributed to the freezing of interfacial and bulk water in the pores. Thus, despite various studies, as mentioned above, it is still questionable whether the anomaly in the supercooled confined water is to be ascribed to the LDW–HDW transition or to other phenomena, such as a fusion affected by the pore surfaces.

Copper rubeanate  $\text{H}_2\text{C}_2\text{N}_2\text{S}_2\text{Cu}$ , investigated in this work, is a type of porous coordination polymer, sometimes called a metal–organic framework. It consists of Cu(II) dimers and dithiooxamide, as shown in Scheme 1, and is denoted as  $\text{H}_2\text{dtoaCu}$ . The pore size of this material is estimated to be 0.6 nm from a nitrogen adsorption measurement.<sup>10</sup> This pore size is much smaller than those of the various porous materials mentioned above (>1 nm).  $\text{H}_2\text{dtoaCu}$  adsorbs water molecules as a function of relative humidity (RH), and the chemical

\* Corresponding author. Phone: +81 4 7136 3494. Fax: +81 4 7134 6069. E-mail: yamamuro@issp.u-tokyo.ac.jp.

<sup>†</sup> University of Tokyo.

<sup>‡</sup> Kyusyu University.

<sup>§</sup> JST-CREST.

<sup>⊥</sup> Kyoto University.

formula reaches  $\text{H}_2\text{dtoaCu} \cdot 3.7\text{H}_2\text{O}$  at RH = 100%. Another important aspect of copper rubeanate is that it has a proton conductivity that is enhanced by  $10^4$  times by adsorbing water in the pore. The conductivity at RH = 100% is 0.01 S/cm, which is as large as that of Nafion membrane,<sup>10</sup> known as the best commercial proton conductor. Despite a great deal of potential in industry, the basic properties of  $\text{H}_2\text{dtoaCu}$  have not been studied well.

In this study, we have investigated the phase behavior and structures of  $\text{H}_2\text{dtoaCu} \cdot n\text{H}_2\text{O}$  with varying water contents,  $n = 0, 2.1, 3.7$ , by adiabatic calorimetry and  $n = 0, 3.7$ , by neutron diffraction. To add to the study of confined water, it is meaningful to investigate the properties of water in the pores with different size and surface conditions from those of previously investigated materials. Of course, the present work should contribute to elucidate the proton-conducting mechanism of this material, especially on the role of water molecules in the pores.

## II. Samples and Experiments

Copper rubeanate was prepared by simple mixing of a dithioxamide aqueous solution and a copper sulfate solution, as described elsewhere.<sup>10</sup> The copper rubeanate hydrates were prepared by putting the samples in a glovebag with RH = 100%. The extent of hydration was adjusted by exposure time; i.e., 5 h for less hydrated samples and 2 days for the fully hydrated sample. The hydration number was precisely determined by weighing the hydrate and comparing with the weight of the dry sample. The completely dry sample was held under vacuum at 50 °C for 24 h. The samples used in this study were  $\text{H}_2\text{dtoaCu} \cdot n\text{H}_2\text{O}$  ( $n = 0, 2.1, 3.7$ ).

The heat capacity measurements were performed using a custom-built adiabatic calorimeter.<sup>11</sup> The precision and accuracy of the heat capacity measurement ( $\Delta C_p/C_p$ ) are 0.05 and 0.2%, respectively. The samples were wrapped with a film of copolymer of tetrafluoroethylene and hexafluoropropylene to avoid reactions between the sample and the sample cell. The wrapped samples were then loaded into the sample cell with helium gas for heat exchange, and the cell was sealed with an indium gasket. The temperature range for the  $C_p$  measurements was from 5 to 285 K.

For the neutron powder diffraction experiments,  $\text{H}_2\text{dtoaCu}$  was deuterated by repeating the following procedure three times; that is, the dried  $\text{H}_2\text{dtoaCu}$  was kept in a saturated heavy water atmosphere for a day and was dried under vacuum for a day. The extent of deuteration reached 98%.  $\text{D}_2\text{dtoaCu} \cdot 3.7\text{D}_2\text{O}$  was prepared by adsorbing heavy water.

The neutron powder diffraction experiments were performed on the powder diffractometer called HERMES, which was constructed by the Institute for Materials Research, Tohoku University. This instrument is installed at the T1-3 port of the JRR-3 reactor in Japan Atomic Energy Agency, Tokai, Japan.<sup>12</sup> Neutrons with a wavelength of 0.182 nm, which were obtained using the (331) reflection of the Ge monochromator, were used. The samples  $\text{D}_2\text{dtoaCu}$  and  $\text{D}_2\text{dtoaCu} \cdot 3.7\text{D}_2\text{O}$  were sealed in vanadium sample cans with indium gaskets. The cans were mounted on the cold head of a closed cycle He-gas refrigerator. The  $\text{D}_2\text{dtoaCu} \cdot 3.7\text{D}_2\text{O}$  sample was measured in the temperature range from 100 to 340 K. The dried  $\text{D}_2\text{dtoaCu}$  sample was measured at room temperature.

## III. Results and Discussion

**Adiabatic Calorimetry.** Figure 1 shows the heat capacities of  $\text{H}_2\text{dtoaCu} \cdot n\text{H}_2\text{O}$  ( $n = 0, 2.1, 3.7$ ). The dried sample

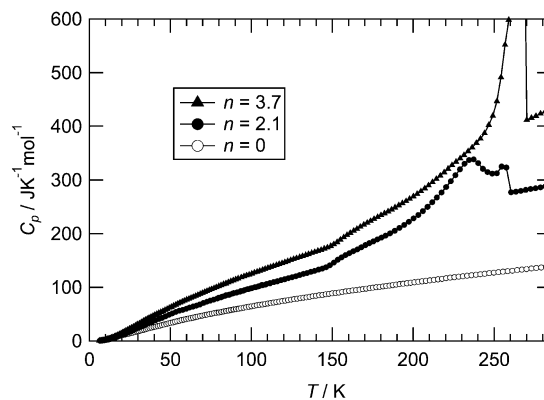


Figure 1. Heat capacities of  $\text{H}_2\text{dtoaCu} \cdot n\text{H}_2\text{O}$  ( $n = 0, 2.1, 3.7$ ).

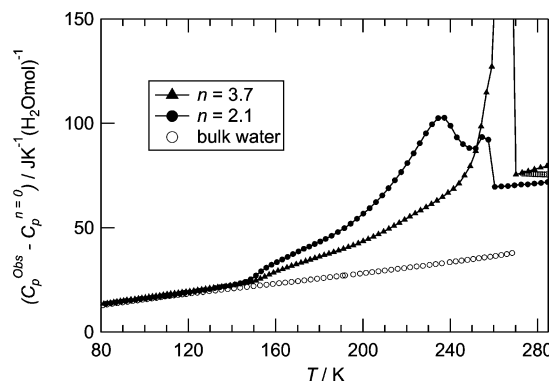


Figure 2. Heat capacities of water adsorbed in  $\text{H}_2\text{dtoaCu}$ .

$\text{H}_2\text{dtoaCu}$  ( $n = 0$ ) exhibited no anomaly, but the hydrate ones,  $\text{H}_2\text{dtoaCu} \cdot n\text{H}_2\text{O}$  ( $n = 2.1, 3.7$ ), showed both a glass transition and a broad first-order transition. The first-order nature of the transition was confirmed from spontaneous endothermic temperature drift under adiabatic conditions. The glass transition temperature was 150 K for the hydrate samples. The temperature and shape of the first-order transition depend on the hydration number, that is, a broad double peak (230 and 255 K) transition for  $n = 2.1$  and a fairly sharp single peak (260 K) transition is observed for  $n = 3.7$ . No anomaly was observed at the fusion temperature of ice, 273.15 K.

The above results indicate that both the glass transition and first-order transition originate from the adsorbed water. The glass transition temperature was close to that of vitreous water prepared by vapor deposition, 135 K.<sup>13</sup> This indicates that the glass transition is due to the freezing of the motions of water molecules in the pores. For the first-order transition, the transition temperature increased, and the peak shape became sharper with increasing water content. It is noteworthy that these tendencies are similar to those observed for water in silica-gels measured by Oguni et al.<sup>9</sup>

Heat capacities of the adsorbed water were calculated by

$$[C_p(n = 2.1 \text{ or } 3.7) - C_p(n = 0)]/n \quad (1)$$

by assuming the additivity of heat capacity. These quantities are plotted in Figure 2 and compared to the heat capacity of bulk water.<sup>14</sup> Below the glass transition temperature, the heat capacities of the hydrate samples almost agree with that of bulk water.<sup>14</sup> These results indicate that the vibrational state of the adsorbed water is almost the same as that of bulk water in the solid state.

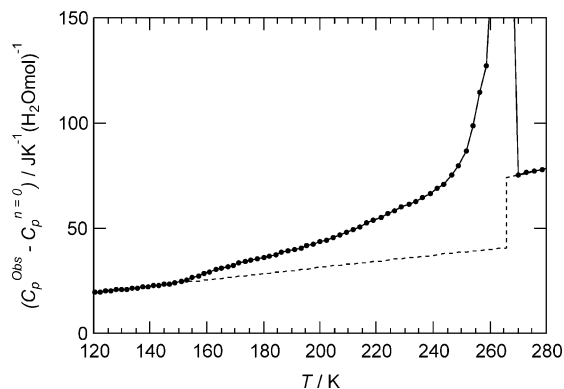


**Figure 3.** Heat capacities of water adsorbed in  $\text{H}_2\text{dtoCu} \cdot 3.7\text{H}_2\text{O}$ . The dashed line represents the baseline for the transitions. See text for the details.

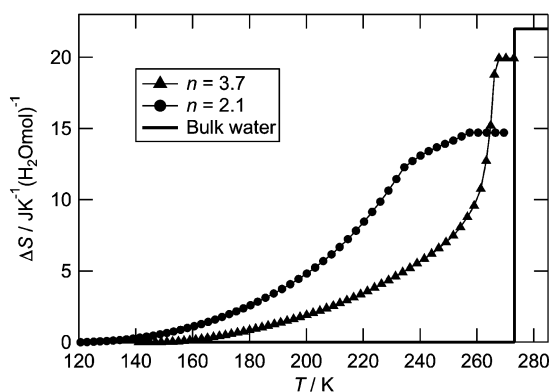


**Figure 4.** Excess entropies of water adsorbed in  $\text{H}_2\text{dtoCu} \cdot \text{H}_2\text{O}$  and bulk water.

To estimate the excess entropy for each transition, the baselines were determined by fitting the heat capacities below the glass transition temperature and above the first-order transition temperature to a second-order polynomial function and a straight line, respectively. These are the simplest polynomial functions to fit the  $C_p$  data in these regions. Each baseline was extrapolated to the peak top temperature ( $T_{\text{trs}}$ ) of the first-order transition, as shown in Figure 3. For the sample with  $n = 2.1$ ,  $T_{\text{trs}}$  was assumed to be the peak top temperature of the main peak, 237.27 K. The transition entropy was calculated as a function of temperature, as shown in Figure 4. It is remarkable that most of the excess entropy occurs below  $T_{\text{trs}}$ . The transition entropy depends on temperature when the baselines below and above  $T_{\text{trs}}$  are not continuous, as in the present case. Therefore, we chose the fusion temperature of bulk water (273.15 K) as the reference temperature to compare the excess entropies of the two hydrate samples ( $n = 2.1$  and 3.7) and bulk water with different transition temperatures. The transition entropy at the reference temperature (273.15 K) was calculated by the equation,

$$\Delta S(273.15 \text{ K}) = \int_{T_i}^{T_{\text{trs}}} [C_p - C_p(\text{LT})]/T \, dT + \int_{T_{\text{trs}}}^{T_f} [C_p - C_p(\text{HT})]/T \, dT + \int_{T_{\text{trs}}}^{273.15 \text{ K}} [C_p(\text{HT}) - C_p(\text{LT})]/T \, dT \quad (2)$$

where  $T_i$  and  $T_f$  are initial and final temperatures of the first-order transition, respectively, and  $C_p(\text{LT})$  and  $C_p(\text{HT})$  are baselines of low- and high-temperature regimes, respectively. The calculated values are listed in Table 1. It is of interest that

**TABLE 1: Transition Entropy of  $\text{H}_2\text{dtoCu} \cdot n\text{H}_2\text{O}$  at the Reference Temperature 273.15 K**

	$T_{\text{trs}}/\text{K}$	$\Delta S(273.15 \text{ K})/\text{J K}^{-1} (\text{H}_2\text{O mol})^{-1}$
$n = 2.1$	$237.27 \pm 0.01$	$19.4 \pm 0.2$
$n = 3.7$	$266.08 \pm 0.01$	$20.8 \pm 0.2$
bulk water	$273.15 \pm 0.01$	$22.0 \pm 0.2$

$\Delta S(273.15 \text{ K})$  of  $n = 2.1$  and 3.7 were similar to the entropy of fusion of bulk water. The present result strongly indicates that the adsorbed water molecules are disordered as large as bulk water at 273.15 K, even though they are hindered by the surface of the pore. The disordered water molecules become ordered through the broad first-order transition on cooling. It is to be noted that some portion of disorder is frozen-in at the glass transition temperature, 150 K. If the water molecules keep on ordering even below 150 K, if the water molecules are not frozen below 150 K, the  $\Delta S(273.15 \text{ K})$  of the hydrate samples may become more close to the entropy of fusion of bulk water because the contribution from the excess heat capacity below 150 K is added.

**Neutron Diffraction.** Figure 5 shows neutron powder diffraction patterns of  $\text{D}_2\text{dtoCu} \cdot 3.7\text{D}_2\text{O}$  and  $\text{D}_2\text{dtoCu}$  (bottom). For  $\text{D}_2\text{dtoCu} \cdot 3.7\text{D}_2\text{O}$ , the temperature dependence of the diffraction pattern was precisely examined across the transition temperature 260 K. Both  $\text{D}_2\text{dtoCu} \cdot 3.7\text{D}_2\text{O}$  and  $\text{D}_2\text{dtoCu}$  exhibited broad patterns without Bragg peaks, indicating that the structures were amorphous. No drastic change of the diffraction pattern (e.g., appearance of Bragg peaks) was observed, even below the first-order transition temperature. It is surprising that the ordering transition observed in the  $C_p$  measurement is so sharp, even though the structure of copper rubenate is amorphous and no evidence of icelike structure is observed below  $T_{\text{trs}}$ . These results imply that the first-order transition is not due to a simple crystallization but to a type of liquid–liquid transition.

Since the data quality is not sufficient and the contribution from the adsorbed water is small, the contribution from the

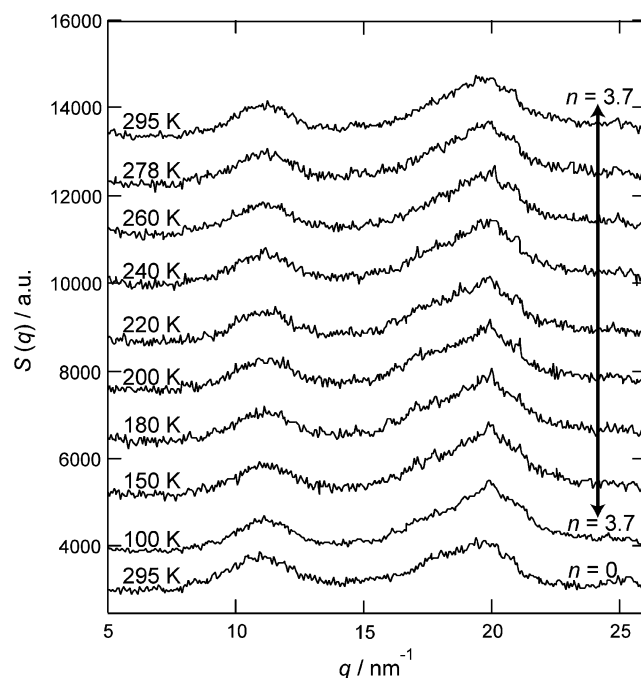


**Figure 5.** Neutron powder diffraction patterns of  $\text{D}_2\text{dtoCu} \cdot 3.7\text{D}_2\text{O}$  and  $\text{D}_2\text{dtoCu}$  (bottom). Each diffraction pattern is shifted upward by 1000.

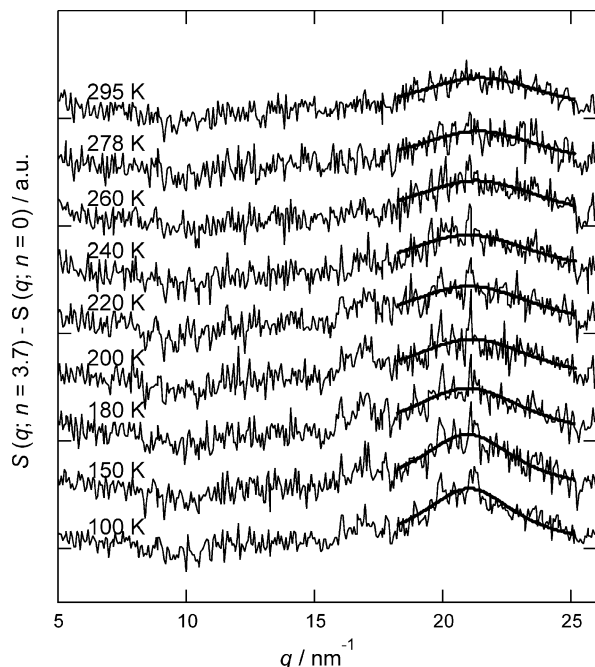


**Figure 6.** Difference in neutron powder diffraction patterns between  $D_2dtoaCu \cdot 3.7D_2O$  and  $D_2dtoaCu$  ( $n = 0$ ). Curves are the results of fitting to Lorentz functions. See text for the details.

adsorbed water was roughly estimated by subtracting the pattern of  $D_2dtoaCu$  from that of  $D_2dtoaCu \cdot 3.7D_2O$ . Here, the cross terms between  $D_2O$  and  $D_2dtoaCu$  are neglected by assuming that the correlation between the adsorbed water and the surface of the pores is not significant. However, the cross terms are sometimes important, as suggested by R. Mancinelli and co-workers.<sup>15</sup> More precise diffraction experiment by using a liquids diffractometer is needed for the conclusive discussion.

Figure 6 shows the temperature dependence of the contribution of the adsorbed water. The data have a large statistical error, since the contribution of the adsorbed water was about 5% of the total scattering intensity. Despite this large error, a broad peak appeared around  $21 \text{ nm}^{-1}$ , which is close to the position of the first sharp diffraction peak (FSDP) of bulk water ( $19 \text{ nm}^{-1}$ ). We regard this peak to be the FSDP of the adsorbed water.

The peaks around  $21 \text{ nm}^{-1}$  were fitted to Lorentzian functions. The fitting was good enough, as shown in Figure 6. The half width at half-maximum (HWHM) and the peak position, both determined by the fitting, are shown as functions of temperature in Figure 7. On heating the sample, the HWHM gradually increased from 150 K and became almost constant above 220 K. This result indicates that the correlation length, roughly estimated by  $(2\pi/\text{HWHM})$ , decreased from 2.7 nm ( $T < 150 \text{ K}$ ) to 1.7 nm ( $T > 220 \text{ K}$ ). The correlation length determined by the same method for bulk supercooled water at 258 K is 1.5 nm, which is close to the value at the higher temperature region of the adsorbed water in the pore. It is of interest that the HWHM is almost constant above 220 K. This can be related to the strong–fragile transition suggested by the previous studies, but it is tough to discuss more because of the poor data quality and rough analysis. In the heating direction, the peak position, roughly corresponding to intermolecular distance, shifted to the high  $q$  direction rather drastically around 260 K. Thus, the peak position more directly reflects the mechanism of the 260 K transition than peak width.

The mechanism of the transition at 260 K speculated from the present results is as follows. The adsorbed water molecules

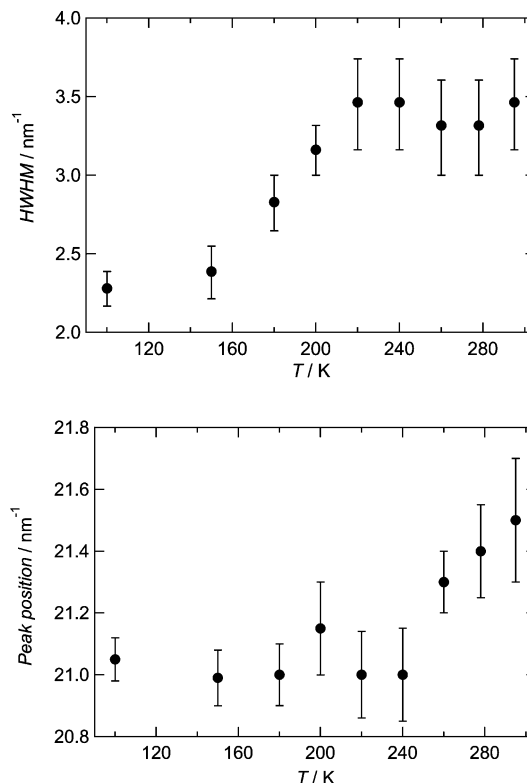


**Figure 7.** Temperature dependence of HWHM and the position of the  $21 \text{ nm}^{-1}$  peak of  $D_2dtoaCu \cdot 3.7D_2O$ .

as well as those in bulk water are disordered above 273 K. They condense on the surface of the pore through the transition on cooling. It should be noted that they are still in a liquid state, since there are no diffraction peaks in Figure 5. Then the water molecules are gradually ordered on further cooling below 260 K, and finally, the water molecules are frozen-in at a mostly ordered state at the glass transition temperature 150 K.

We consider that the transition found at 260 K in this study is different from the strong-fragile transition investigated mainly by previous quasielastic neutron scattering.<sup>6–8</sup> This is supported also by the fact that the transition temperature of the strong–fragile transition is usually around 220 K and tends to be lowered by the hydrophobic interaction. Anyhow, more precise data and careful analysis are required for the conclusive discussion on the mechanism of the transition.

Finally, we discuss the relation between the proton-conductivity and the calorimetric and structural data obtained in this work. In copper rubeanate hydrates, it is sure that the water molecules are carriers of protons. The highly disordered configuration of the adsorbed water, corresponding to large entropy due to the transition, should be related to high mobility of the water molecules and a resulting high proton conductivity of copper rubeanate hydrates. Another important aspect is that copper rubeanate exhibits amorphous structure, indicating that the pores are partly broken and connected to each other, as in the case of the Nafion membrane. It is desirable to measure proton conductivity across the transition temperature of 260 K to clarify the effect of the configurational disorder of the water molecules.

#### IV. Conclusion

In this paper, the phase behaviors and structures of copper rubeanate hydrates were investigated by adiabatic calorimetry and neutron diffraction. The dry sample has an amorphous



structure and no transition. The hydrated samples, which also have an amorphous structure, exhibit a glass transition and a broad first-order transition due to the adsorbed water molecules around 150 and 260 K, respectively. The transition entropy was similar to the entropy of fusion of bulk water, indicating that the disorder of the adsorbed water is similar to that of bulk water above the transition temperature. The position and width of the neutron diffraction peak owing to the adsorbed water exhibited steplike changes around the transition. From the above results, we speculate that the transition at 260 K is a liquid–liquid transition due to the condensation of water on the surface of the nanopores, and the condensed water molecules are gradually ordered below 260 K and frozen-in at the glass transition around 150 K.

**Acknowledgment.** The authors thank Professor Kenji Ohoyama (Tohoku University) for his help in the neutron diffraction experiments on HERMES. This work is financially supported by the Core Research of Evolutional Science & Technology program (CREST) from the Japan Science and Technology Agency (JST).

## References and Notes

- (1) Speedy, R. J.; Angell, C. A. *J. Chem. Phys.* **1976**, *65*, 851–858.
- (2) Sastry, S.; Debenedetti, P. G.; Sciortino, F.; Stanley, H. E. *Phys. Rev. E* **1996**, *53*, 6144–6154.
- (3) Mishima, O.; Stanley, H. E. *Nature* **1998**, *396*, 329–335.
- (4) Mishima, O. *J. Chem. Phys.* **1994**, *100*, 5910–5913.
- (5) Soper, A. K.; Ricci, M. A. *Phys. Rev. Lett.* **2000**, *84*, 2881–2884.
- (6) Liu, L.; Chen, S.-H.; Faraone, A.; Yen, C.-W.; Mou, C.-Y. *Phys. Rev. Lett.* **2005**, *95*, 117802–117805.
- (7) Yoshida, Y.; Yamaguchi, T.; Kittaka, S.; Bellissent-Funel, M.-C.; Fouquet, P. *J. Chem. Phys.* **2008**, *129*, 054702–054712.
- (8) Chu, X.-Q.; Kolesnikov, A. I.; Moravsky, A. P.; Garcia-Sakai, V.; Chen, S.-H. *Phys. Rev. E* **2007**, *76*, 021505–021510.
- (9) Oguni, M.; Maruyama, S.; Wakabayashi, K.; Nagoe, A. *Chem. Asian J.* **2007**, *2*, 514–520.
- (10) Kitagawa, H.; Nagao, Y.; Fujishima, M.; Ikeda, R.; Kanda, S. *Inorg. Chem. Commun.* **2003**, *6*, 346–348.
- (11) Yamamuro, O.; Oguni, M.; Matsuo, T.; Suga, H. *Bull. Chem. Soc. Jpn.* **1987**, *60*, 1269–1275.
- (12) Ohoyama, K.; Kanouchi, T.; Nemoto, K.; Ohashi, M.; Kajitani, T.; Yamaguchi, Y. *Jpn. J. Appl. Phys.* **1998**, *37*, 3319–3326.
- (13) Sugizaki, M.; Suga, H.; Seki, S. *Bull. Chem. Soc. Jpn.* **1968**, *41*, 2591–2599.
- (14) Haida, O.; Matsuo, T.; Suga, H.; Seki, S. *J. Chem. Thermodyn.* **1974**, *6*, 815–825.
- (15) Mancinelli, R.; Imberti, S.; Soper, A. K.; Liu, K. H.; Mou, C. Y.; Bruni, F.; Ricci, M. A. *J. Phys. Chem. B* **2009**, *113*, 16169–16177.

JP912212M